Implementation of saturation for modelling pattern noise using naturalistic stimuli

Sreeja Rajesh[a,b,c], Tamath Rainsford[a,c], Russell S. A Brinkworth[b,c], Derek Abbott[a,c] and David C. O'Carroll[b,c]

[a]School of Electrical & Electronic Engineering, The University of Adelaide, SA 5005, Australia.
[b]School of Molecular and Biomedical Science, The University of Adelaide, SA 5005, Australia.
[c]Centre for Biomedical Engineering, The University of Adelaide, SA 5005, Australia.

ABSTRACT

Insects with their amazing visual system are able to perform exceptional navigational feats. In order to understand how they perform motion detection and velocity estimation, much work has been done in the past 40 years and many models of motion detection have been proposed. One of the earliest and most prominent models is the Reichardt correlator model. We have elaborated the Reichardt correlator model to include additional non-linearities that mimic known properties of the insect motion pathway, including logarithmic encoding of luminance and saturation at various stages of processing. In this paper, we compare the response of our elaborated model with recordings from fly HS neurons to naturalistic image panoramas. Such responses are dominated by noise which is largely non-random. Deviations in the correlator response are likely due to the structure of the visual scene, which we term *Pattern noise*. Pattern noise is investigated by implementing saturation at different stages in our model and comparison of each of these models with the physiological data from the fly is performed using cross covariance technique.

Keywords: Reichardt correlator, pattern noise, saturation, artificial insect vision

1. INTRODUCTION

Insects with their relatively simple visual system can outperform any man-made flying system. This is clearly obvious if you observe a fly making a perfect landing on a leaf swaying in the wind, a group of bees flying together at top speed without colliding into one another or, an insect hovering near a flower. The amazing navigational ability of insects has fascinated scientists, motivating a number of biologically inspired models of motion detection[1–8] over the past four decades. Most of these models are spatiotemporal energy models, the dominant models for motion detection in vertebrates, and are mathematically equivalent to correlator models.[9] Correlator models have been applied to explain not only motion detection in insects but also in humans, birds and cats.[10–12]

The Reichardt covariance motion detector[13] possess a highly parallel architecture. Each elementary motion detector (EMD) detects motion in a preferred direction by comparing a signal from one receptor with a delayed signal from an adjacent receptor. The comparison is performed using a nonlinear, multiplicative interaction

Further author information: (Send correspondence to Sreeja Rajesh)
Sreeja Rajesh, e-mail: srajesh@eleceng.adelaide.edu.au, Telephone: 8303-6296
Tamath Rainsford, e-mail: tamath@eleceng.adelaide.edu.au
Russell Brinkworth, e-mail: russell.brinkworth@adelaide.edu.au
Derek Abbott, e-mail: dabbott@eleceng.adelaide.edu.au
David O'Carroll, e-mail: david.ocarroll@adelaide.edu.au

Smart Structures, Devices, and Systems III, edited by Said F. Al-Sarawi, Proc. of SPIE
Vol. 6414, 641424, (2007) · 0277-786X/07/$15 · doi: 10.1117/12.696105

between the two channels. Two EMDs tuned to opposite directions are combined to form a bidirectional motion detector.

Though both insects and humans are capable of reliably estimating image velocities,[14, 15] the basic correlator model does not function as a reliable velocity estimator. It accurately indicates the directional motion of sinusoidal gratings, but the response depends on contrast (brightness) and spatial frequency (shape) as well as velocity.[16] Analysis and simulations suggest that the processes commonly found in visual systems, such as pre-filtering, response compression, integration, and adaptation, improve the reliability of velocity estimation and expand the range of velocities that can be coded.[17–23]

In this paper, using our elaborated Reichardt model, we model the response of fly EMD array's to naturalistic images moving at constant velocity. Differences in the local structure of various natural images result in deviations in the correlated response of local detectors, which we term pattern noise. Natural images are far from random and show a large degree of structure. This structure can be described by the statistics of the image source, and can be considered as prior knowledge. Therefore a certain amount of image data is predictable and thus redundant.[24, 25] The visual system of the fly appears to be optimized to take advantage of the statistical properties of natural images using specific optimization criteria of redundancy minimization, maximisation of information transmission, sparseness of the neural coding and minimising reconstruction error, demonstrating that simple optimisation principles combined with knowledge of image statistics can predict visual processing strategies that are found in nature.[26] We investigate this pattern noise through both electrophysiology in our model insect animal *Eristalis tenax* and with our elaborated Reichardt model.

It is found that the implementation of compressive non-linearity (saturation) in our model has a tremendous effect on the shape of the pattern noise. So we investigate the influence of saturation at different positions in our model and we compare the shapes of the fly response with that of our model using cross covariance method. We have also discussed the performance of each model with respect to pattern noise using the Relative error measure.

2. MODELLING OF A MOTION DETECTOR USING REICHARDT CORRELATOR MODEL

Figure 1 shows a simplified version of the Reichardt correlator model. Receptors A and B are separated by an angular distance $\Delta\phi$. The signal from A is temporally delayed by the low-pass filter D before multiplication by the signal from B. This multiplication produces a positive output in response to rightward image motion. To achieve similar sensitivity to leftward motion and to cancel excitation by stationary flickering stimuli, a parallel delay-and-multiply operation takes place on the opposite arm. The outputs of the two multiplications are subtracted to give a single time-dependent correlator output R.

Although the correlator is nonlinear, its response to sinusoidal stimuli is of interest. If the input is a sinusoidal grating that contains only a single frequency component, the oscillations of the two subunits cancel and the correlator produces a constant output. For any linear delay filter, the output level depends separably on spatial and temporal frequency.[16] If the delay filter D is a first order low pass with time constant τ, a sinusoid of amplitude C and spatial frequency f_s travelling to the right at velocity v produces an output $R(t)$as described in equation (1).

$$R(t) = \frac{C^2 f_t}{2\pi\tau f_t^2 + 1/(2\pi\tau)^2} \sin(2\pi f_s \Delta\phi) \tag{1}$$

where f_t is the temporal frequency of the input signal.[16] At a given spatial frequency, the magnitude of correlator output increases with temporal frequency up to an optimum $f_{t,\mathrm{opt}} = 1/(2\pi\tau)$ and then decreases monotonically as the velocity continues to increase. The output also varies with the square of C, which specifies grating brightness or, in the presence of preprocessing stages, grating contrast. A physical luminance grating must have positive mean luminance, so it will contain a dc component as well as an oscillatory component. In this case, the output will oscillate about the level given by Eq. (1).

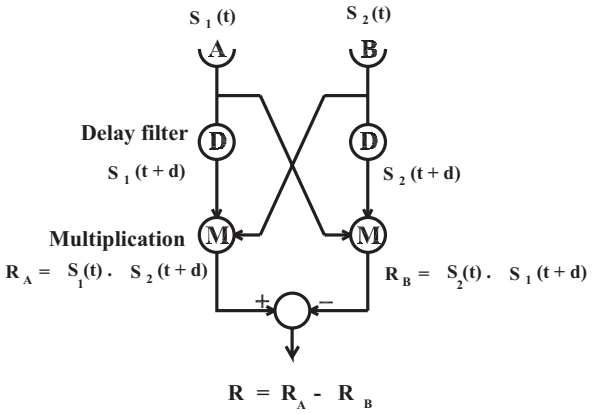

Figure 1. The Reichardt correlator has two receptors A and B that take two input signals s_1 and s_2 with a fixed angular separation $\Delta\phi$. Each of these time dependent inputs passes through a linear delay filter (D) before being multiplied by the other, undelayed signal. The results of the two correlations thus obtained R_A and R_B are subtracted to produce a single output R. An object moving to the right will produce a positive output; an object moving to the left will produce a negative output.

3. ELABORATIONS TO THE REICHARDT CORRELATOR MODEL

Although the simple correlator model is able to detect motion very well, it is not a good velocity estimator. this is because the response depends on the spatial structure of the image and on the contrast. In an attempt to make the response independent of contrast and spatial frequency, we have elaborated the basic EMD model. Previous work shows that addition of various spatial and temporal pre-filtering, integration and adaptation mechanisms improve the performance of the correlator model.[27] In our elaborated model, in order simplify it for error analysis, we have not included motion adaptation. The spatial low pass filtering is implemented using a Gaussian filter of half width 2° and the temporal bandpass filter is implemented using a log-normal difference filter.[28]

In our experiments, the natural images, shown in Figure 2, were photographed from favored hovering positions of the hoverfly. Then the edges of the images are wrapped to form a panoramic image, which is given as a stimulus to our fly EMD model. A panorama is formed by 'warping' 12 image 'tiles' at 30° intervals to remove lens distortion and then wrapping its ends together. This was achieved using Apple Quicktime VR Authoring Studio. The naturalistic three images which we have chosen differ in aggregated natural contrast (global contrast) approximately by a factor of 3 (Image 1 has a global contrast, $Cn = 0.65$, Image 2 has $Cn = 1$ and for Image 3, $Cn = 0.38$ as calculated by Straw[29]).

Figure 2. A panorama of the image is formed by 'warping' 12 image tiles at 30° intervals to remove lens distortions and then by wrapping its ends together using Apple Quicktime VR software on a Macintosh computer.

Spatial pre-filtering is implemented by two-dimensional convolution of the image with a Gaussian kernel of half width of 2°, which approximates the acceptance function of typical fly photoreceptor.[30] Only the luminance (gray scale) information is taken from the image using the green channel, since photoreceptors are green sensitive. The distance between two ommatidia in an insect eye is between 1 and 1.5 degrees. Since the insect is looking at an image of 360 degrees, if we consider the inter-ommatidial angle as 1.5 degrees,[31,32] there will be a total of 240 ommatidia looking at the image. So there will be an array of typically 240 EMDs working together to detect motion as shown in Figure 3.

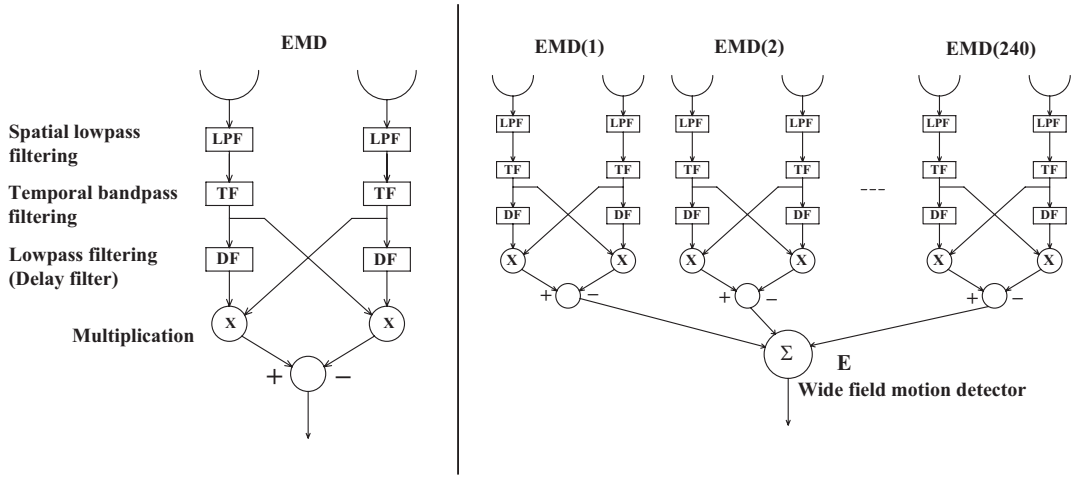

Figure 3. The elaborated EMD array. On the left, we have one elementary motion detector elaborated to include spatial low pass filtering (LPF) using a Gaussian filter of half width 2° and a temporal band pass filter (TF) using a log-normal difference filter is shown. This then passed through the delay and compare mechanism of the Reichardt detector using the the delay filter (DF) which is a low pass filter. On the right we have our EMD array model, where an array of 37 × 240 elaborated EMDs are used to detect motion. The input stimulus given is a panoramic image photographed from a natural environment favored by insects, and considering the inter ommatidial angle as 1.5° there will be typically 240 ommatidia (EMDs) in one horizontal slice working together to detect motion. The output of these EMDs is pooled to get an average output (E) to enable wide field motion detection.

The images in Figure 2 are temporally filtered individually with a difference of log-normal filter to mimic the response of the photoreceptor and lamina monopolar cells.[28,33,34] The temporally pre-filtered image is

then converted to a space-time matrix based on desired velocity. Then based on the height of the image, we have 37 rows of the EMDs computed in the vertical dimension with an inter-ommatidial angle of 1.5 degrees.

The spatio-temporally pre-filtered image is then given to the EMD array, which correlates the inputs to give an array of outputs. Then the EMD array model mimics the lobula by averaging the outputs to produce an average EMD response.

4. EVIDENCE OF PATTERN NOISE — ELECTROPHYSIOLOGICAL RESULTS

Naturalistic panoramic images shown in Figure 2 were displayed on the inside of a virtual cylinder, which was centered on the fly (*Eristalis Tenax*, male) and perspective distorted according to the fly's calibrated 3D position and orientation relative to the CTR. Pure yaw rotations were simulated by spinning the virtual cylinder about a dorsal-ventral axis of the fly's head. The display subtended approximately 90 degrees horizontally from the midline to the lateral portion of the animal, thus stimulating most of the receptive field of the HS neurons.[35]

We chose three naturalistic images that differ in aggregated natural contrast $\bar{C}_n$ approximately by a factor three. In the first set of experiments the three selected images were presented to the insect at a constant speed of 180 degrees per second, which is a value close to the optimal velocity in *Eristalis tenax*.[29] A particular image was presented in eight trials. The stimulus period was long enough for the image to pass the HS cell's receptive field twice completely. From one trial to the next the image's starting position was shifted by 45 degrees, i.e. in the stimulus periods of the seven trials following the first trial the stimulus was phase-shifted by 45, 90, 135, 180, 225, 270, 315 degrees. Figure 4 shows the HS cell's response to such a sequence of naturalistic stimuli at various phase shifts.

The response functions that make up a set of eight trials were aggregated in two different ways. The first is 'time-aligned' response where the response is aligned by stimulus time. Because the initial phase is different in each trial, phase dependent noise (pattern noise) disappears in the average, just as if we had simulated a 360 degree EMD array. The second is 'phase-aligned', where we align each phase-delayed image with the data obtained for phase zero, so that it is the image position that is averaged, rather than time. Averaging in these two different ways produces different results. By comparing the standard deviation of the time aligned responses to that of the phase aligned responses in Figure 4, we can see the 'pattern noise' clearly dominating the phase-aligned response, indicating the impact of spatial structure in naturalistic stimuli on HS cells response to constant velocity.

Physiological motion detectors suffer from random noise, which is due to the variation in its response on repeated presentation of identical stimulus patterns. The random noise experienced by a biological motion detector falls into two categories namely photon noise and intrinsic noise. The photon noise results from variations in the number of photons absorbed by a photoreceptor in a given unit of time. In addition, the neurons and synapses that comprise the correlator generate intrinsic noise. Studies done on the LMCs (Lamina Monopolar Cells) by Laughlin[18] indicates that photon noise dominates intrinsic noise up to moderate light intensities and at higher light intensities, photon noise equals intrinsic noise in magnitude.

Dror conducted studies on photon noise using natural images and found that while photon noise leads to a slight increase in relative error, its contribution is small compared to that of pattern noise suggesting that the performance of a velocity estimation system based on Reichardt correlators depends primarily on responses to pattern noise.[36] The pattern noise here is not a random source of noise. It is most likely due to excitation of individual local detectors which extract motion information. Arrays of such detectors could provide spatially distributed information which is integrated at or before the level of wide field motion sensitive cells such as HS. Spatial pooling from just a single pair of HS cells might be enough to smooth out the pattern noise.

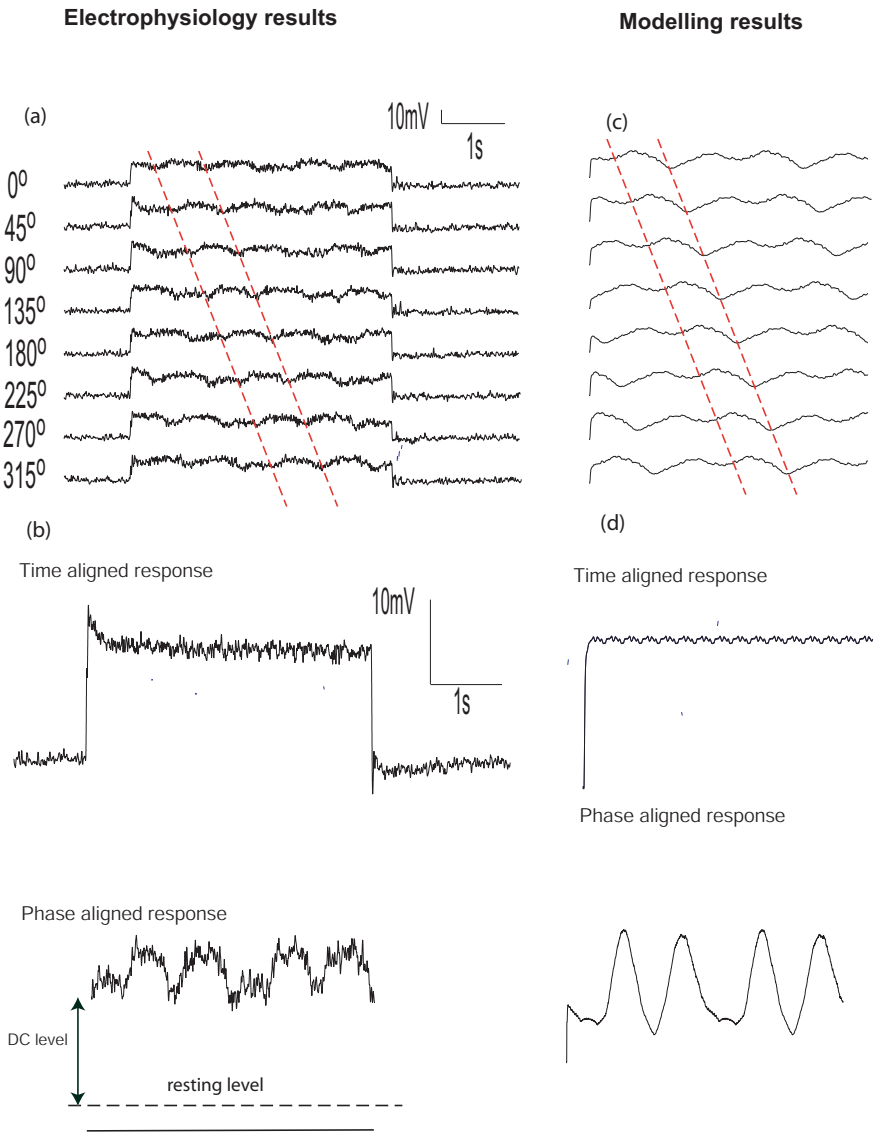

Figure 4. Comparison of physiological and modelling results using the same stimulus at different phases and their phase aligned and time aligned responses. On the left hand side, this figure shows the response of the HS neuron to Image 1, with the image presented moving at 180 degrees per second at 8 different initial phases, each 45 degrees apart. Graph (a)shows the response to each of these 8 configurations. Graph (b) shows the response averaged in two ways, time aligned and phase aligned. In the time aligned method, the normal average of the each of the eight response removes the pattern noise as the response is aligned by stimulus time. In the phase aligned method, we align each phase delayed image with the data obtained for phase zero and then we average it. Now the pattern noise is still present because in this way, it is the image position that is averaged rather than time, and we can still see the noise as the noise is locked in the stimulus position. On the right hand side, this figure shows the modelling results for the same experiment with the same Image 1 using our elaborated Reichardt model. Graph (c) shows the response of our model at 8 different initial positions and part (d) shows the time aligned and phase aligned graphs obtained with our model. In order to further analyze pattern noise, saturation, which is known to present in the fly eye, is added to our model which is discussed in the next section.

4.1. Evidence of Pattern Noise — Modelling Results

We repeated the experiments done in the insect with our elaborated model using the same stimuli, shown in Figure 2, at the same speed of 180 degrees per second. Comparing the phase aligned response of the model with the physiological data in Figure 4, it is seen that the shape of pattern noise differs in the model from that of the response of the HS neuron. This could be because this model has no compressive non-linearity implemented as is known be found in the fly.

4.2. Implementation of Saturation

Both simple and elaborated Reichardt correlators show an increase of response amplitude with stimulus contrast. The neural and behavioral responses of the fly display such a dependence only at very low contrasts. As contrast increases above a few percent, the response begins to level off due to a static, compressive non-linearity, which is termed *contrast saturation*.[36] This is due to limitations in the range of responses that can be signaled by physiological mechanisms.

Saturation of the visual signal first occurs in the photoreceptors, which respond roughly to logarithm of luminance.[18] Saturation reduces relative error partly by reducing contrast difference from one region of the image to another. It is seen in flies that this saturation occurs primarily after linear pre-filtering, but before the multiplication operation indicating that contrast saturation must take place after elimination of the mean light intensity from the signal.[16,36] Saturation is modelled here by including a compressive non-linearity such as a hyperbolic tangent function of the form, $\rho(C) = \tanh(C)$.

It is known that saturation also takes place on both the delayed and undelayed arms of the correlator following the delay filter.[16,36] Based on this, we have implemented compressive nonlinearity before the multiplication operation on both correlator arms. The outputs of the wide field neurons are also found to saturate due to shunting of the membrane potential.[20] This is introduced as a compressive non-linearity following spatial integration.[36] Such an effect will flatten the peaks of the velocity response curves effectively allowing neuron to use more of its dynamic range to signal low velocities. Based on this we have implemented saturation also at the output stage of our model.

When saturation is added at various locations within the model, it has a clear effect on the shape of pattern noise. We have explored the effect of saturation at the photoreceptors (input), at the correlator arms and at the output after spatial integration of the correlator outputs and of various combinations of these as shown in Figure 5.[37]

5. PATTERN NOISE ANALYSIS USING DIFFERENT IMAGES

In order to gain a better understanding of the affect of saturation on pattern noise, we have studied the influence of saturation implemented at different positions of the model in different images. In all the eight cases the phase aligned data, which shows the maximum pattern noise, is compared to the phase aligned physiological data. In order to evaluate and compare each of the modelled response with the fly's response, we calculate the cross covariance value.

We have repeated the experiment using the three different images seen in Figure 2 at the optimum speed of 180deg/sec and at a maximum contrast of 1. The results obtained in each case are shown in the Figures 6, 7 and 8 and the cross covariance values and the relative error values calculated for each case are shown in the Table 1and Table 2 5. Cross covariance is a measure of similarity of two signals. True cross covariance is the cross-correlation of mean-removed sequences. Since we are actually comparing the shape of the two signals we are not interested in the DC value and hence we subtract the DC value before cross correlating it. This results in cross covariance measure which is used here to compare the physiology and modelling response.

The error measure used here called the relative error defined by Dror as, $E_{\text{rel}} = E_{\text{abs}}/\overline{R}$, where the absolute error (E_{abs}) is the difference between the actual response and the expected response.[36] The expected response is the mean response value that is given by $\overline{R}$. For a given set of images, moving at a given velocity, the mean

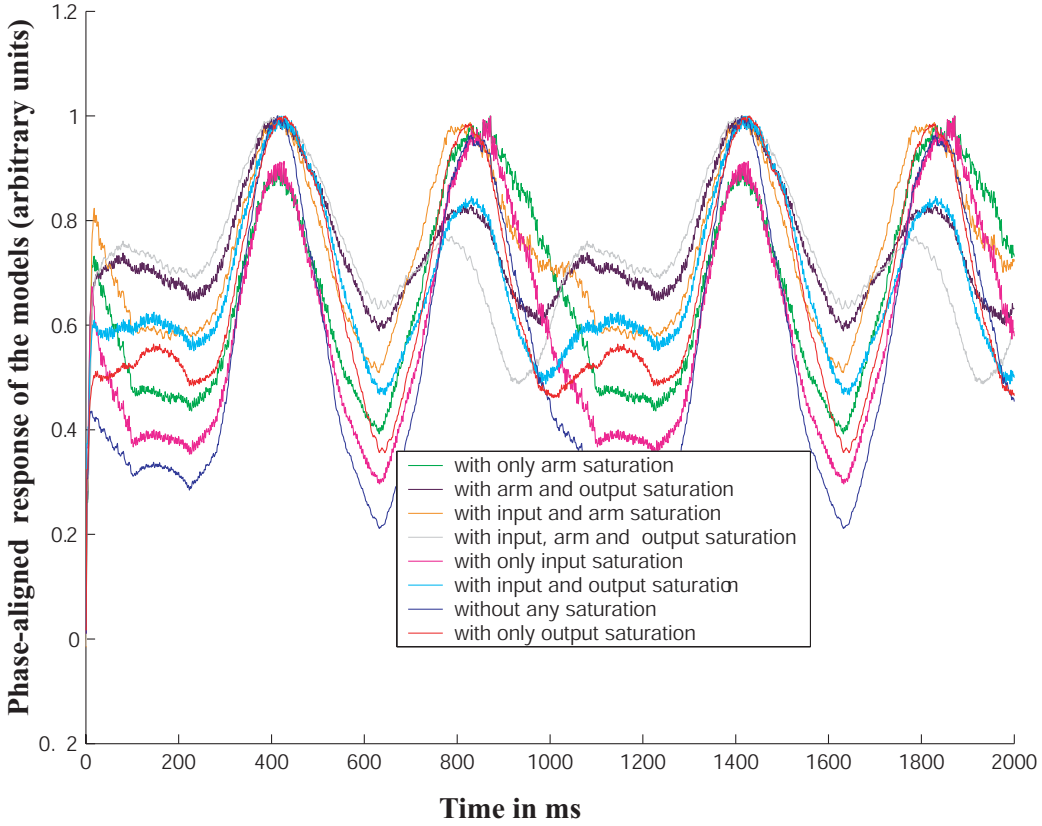

Figure 5. Phase aligned simulation results obtained by running the model at 180 degrees per sec using the disrupted image 1 shown in figure 15 at a contrast of 1. We have implemented saturation at the input stage, at the photoreceptors, at the correlator arms before multiplication and on the mean correlator output individually and also combination of saturation at different places and the phase aligned responses showing the pattern noise in each case is shown here. Note that the saturation implemented at different positions have a clear effect on the shape of the pattern noise indicating that perhaps saturation has a key role in influencing pattern noise in the fly motion pathway.

response $\overline{R}$ is calculated by averaging the response of the wide field correlator at all points in the selected sampled space and sampled time. The relative error for the same set of responses is found by dividing their standard deviation by the mean. In this paper, we evaluated the performance of the model based on its effect on pattern noise.

From the covariance Table 1, it is clear that even though the results of saturation implemented at different positions when superimposed on each other shows a similarity with the physiological data, the cross covariance results tell us a different story. The model with no saturation implemented gives better covariance than models

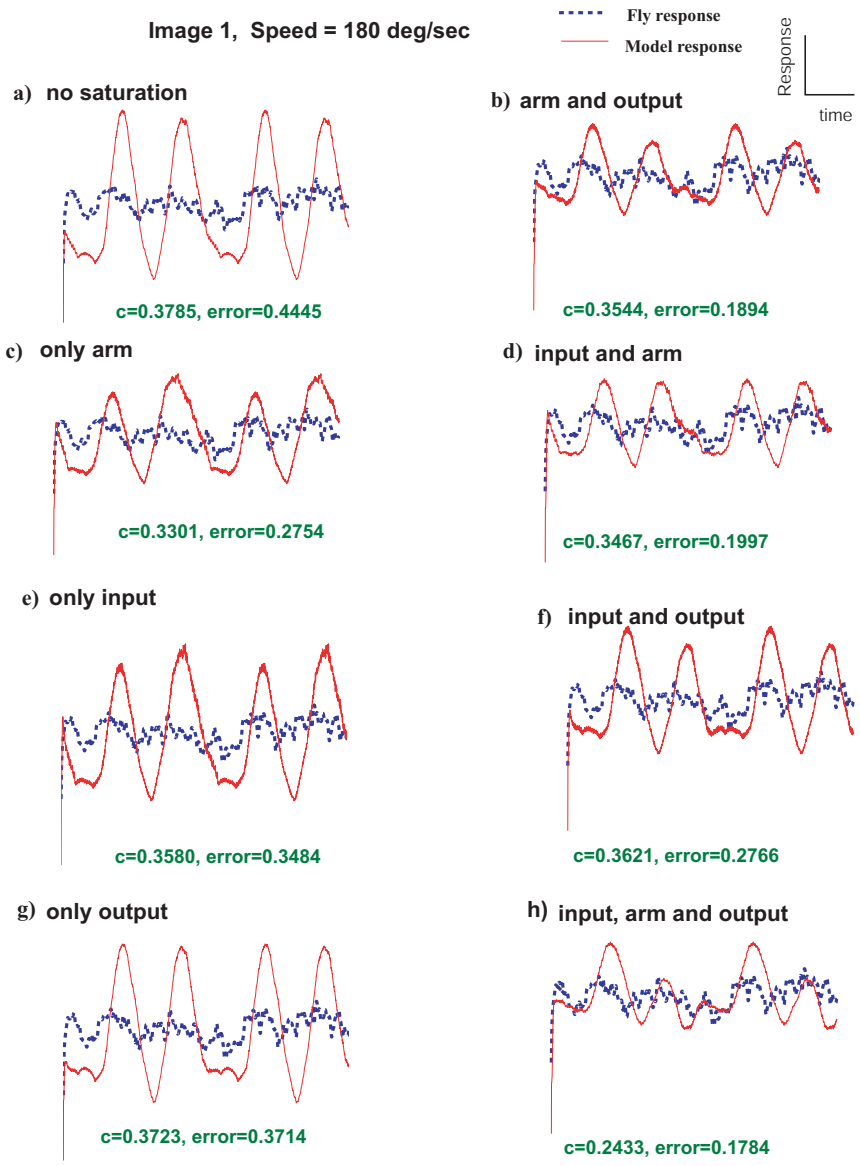

Figure 6. Simulated phase aligned results superimposed with the physiological phase aligned fly response using Image 1. The phase aligned results are obtained by using a stimuli Image 1 moving at a speed of $180 deg/$sec at a contrast of 1. The c values gives the cross covariance values obtained in each case and the R.E values or the error values gives the relative error measured in each case. The experiment is repeated with different models with saturation implemented at different places to compare the shapes of the curves obtained in each case. It is seen that the model with no saturation implemented on it gives the best covariance value. Though we know saturation phenomena exist in the fly eye, and that it has an effect on the shape of pattern noise, the low covariance value shows that there are still more non-linearities present in the fly eye which the model has failed to capture. When we compare relative error, it is seen that implementation of saturation decreases the relative error or pattern noise indicating addition of saturation helps in reducing pattern noise.

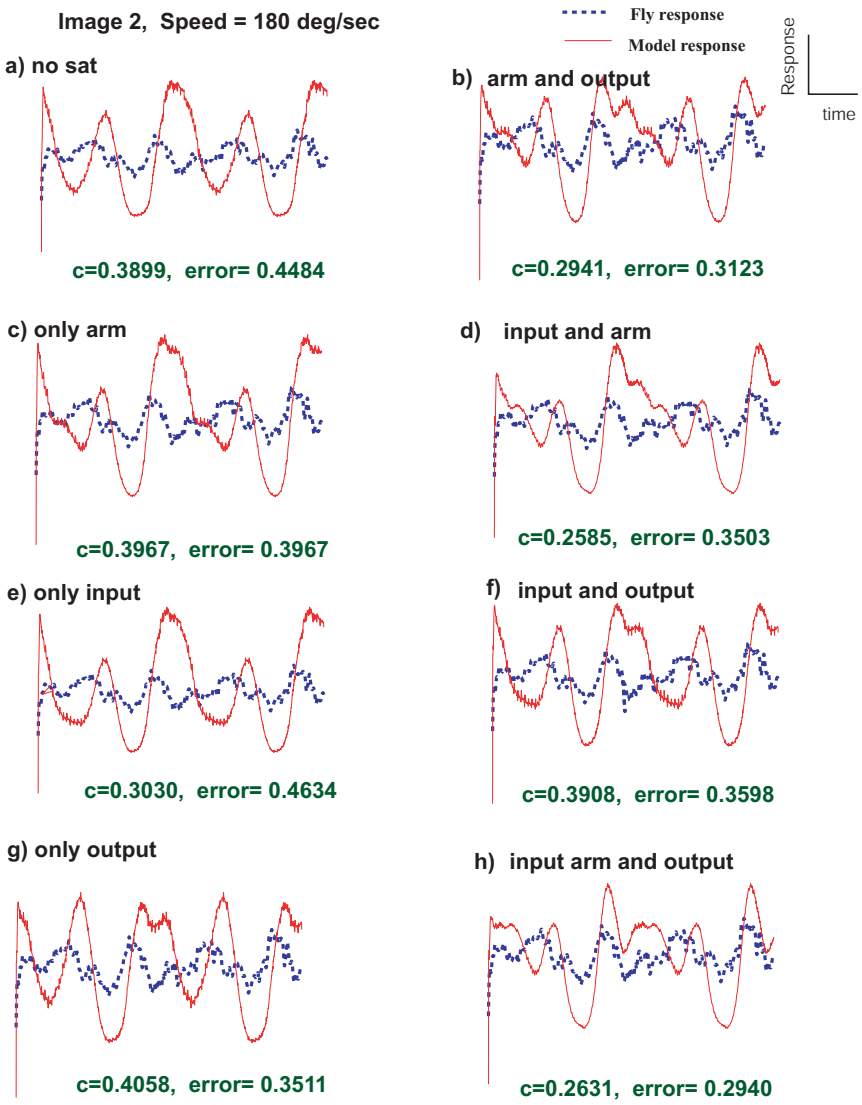

Figure 7. Simulated phase aligned results superimposed with the physiological phase aligned fly response using Image 2. The phase aligned results are obtained by using a stimuli Image 2 moving at a speed of $180 deg/\text{sec}$ at a contrast of 1. The c values gives the cross covariance values obtained in each case and the R.E values gives the relative error measured in each case. The experiment is repeated with different models with saturation implemented at different places to compare the shapes of the curves obtained in each case. It is seen that the model with no saturation implemented on it gives a better result than most of the saturated models. Though we know saturation phenomena exist in the fly eye, and that it has an effect on the shape of pattern noise, the low covariance value shows that there are still more non-linearities present in the fly eye which the model has failed to capture. When we compare relative error, it is seen that implementation of saturation decreases the relative error or pattern noise indicating addition of saturation helps in reducing pattern noise.

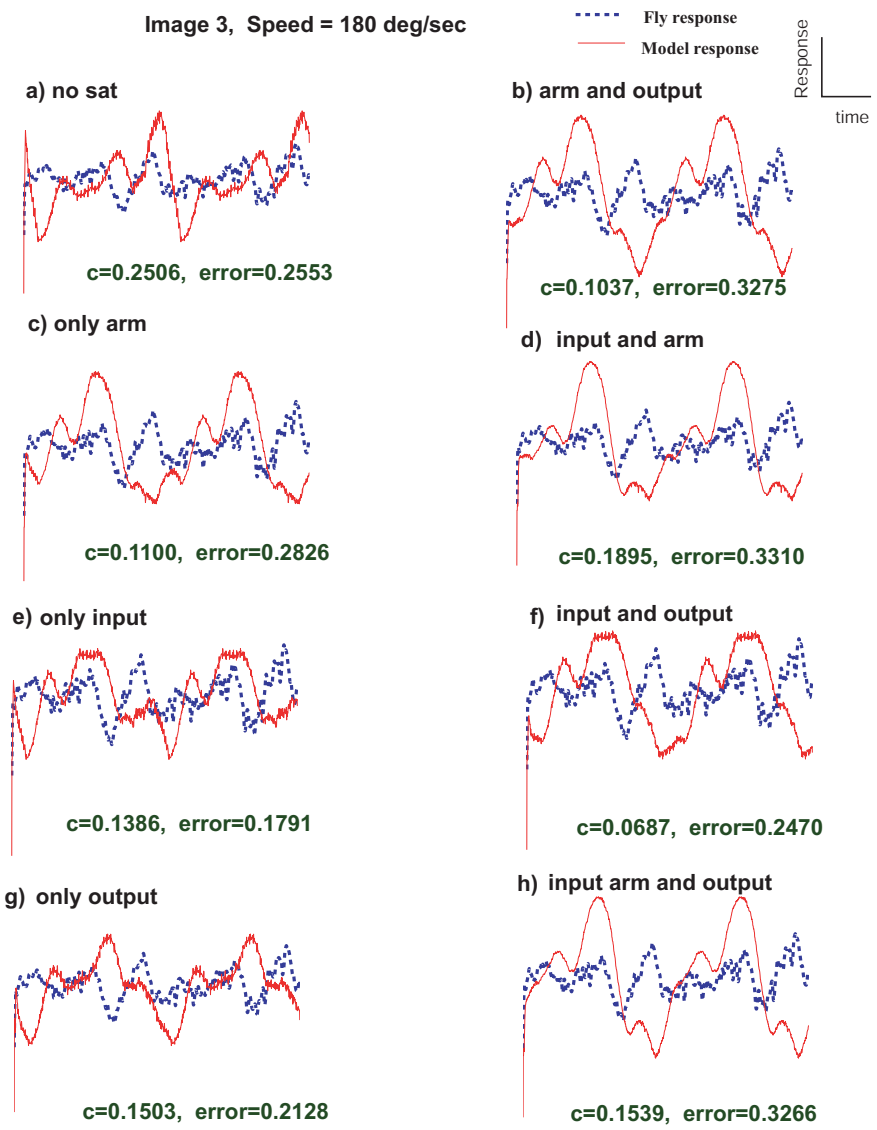

Figure 8. Simulated phase aligned results superimposed with the physiological phase aligned fly response using Image 3. The phase aligned results are obtained by using a stimuli Image 3 moving at a speed of $180 deg/\text{sec}$ at a contrast of 1. The c values gives the cross covariance values obtained in each case and the R.E values gives the relative error measured in each case. The experiment is repeated with different models with saturation implemented at different places to compare the shapes of the curves obtained in each case. It is seen that the model with no saturation implemented on it gives the best covariance results. Though we know saturation phenomena exist in the fly eye, and that it has an effect on the shape of pattern noise, the low covariance value shows that there are still more non-linearities present in the fly eye which the model has failed to capture. When we compare relative error, it is seen that only for this image, which has the lowest aggregated natural contrast[29] when compared to the other two images, the error values have not improved with the addition of saturation.

Model	Image 1	Image 2	Image 3
no saturation	0.3785	0.3899	0.2506
only arm saturation	0.3301	0.2885	0.1100
only input saturation	0.3580	0.3030	0.1386
only output saturation	0.3723	0.4058	0.1503
input and arm saturation	0.3467	0.2585	0.1895
input and output saturation	0.3621	0.3908	0.0687
arm and output saturation	0.3594	0.2941	0.1037
all saturation	0.2433	0.2631	0.1539

Table 1. Cross covariance values for each model. From this Table, it is clear that even though the results of saturation implemented at different positions when superimposed on each other shows a similarity with the physiological data, the cross covariance results tell us a different story. The model with no saturation implemented gives better covariance than models with saturation implemented at different positions. But for the Image 2, the model with just output saturation gives a good covariance value.

Model	Image 1	Image 2	Image 3
no saturation	0.4445	0.4484	0.2553
only arm saturation	0.2754	0.3967	0.2826
only input saturation	0.3484	0.4634	0.1791
only output saturation	0.3714	0.3511	0.2128
input and arm saturation	0.1197	0.3503	0.3310
input and output saturation	0.2766	0.3598	0.2470
arm and output saturation	0.1894	0.3123	0.3275
all saturation	0.1784	0.2940	0.3266

Table 2. Relative error values for each model. From the relative error Table, it is clear models with no saturation gives a higher relative error compared to models with saturation implemented. This is because of the greater difference in magnitude between the unsaturated response and the physiological data. Relative error actually measures the magnitude of the pattern noise and demonstrates that an unsaturated model has greater pattern noise than a model with all saturation. So in terms of relative error, saturation improves the model performance for images 1 and 2. For Image 3, which has the lowest contrast,[29] it is seen that addition of saturation does not reduce pattern noise.

with saturation implemented at different positions. But for the Image 2, the model with just output saturation gives a good covariance value.

From the relative error Table 2, it is clear models with no saturation gives a higher relative error compared to models with saturation implemented. This is because of the greater difference in magnitude between the unsaturated response and the physiological data. Relative error actually measures the magnitude of the pattern noise and demonstrates that an unsaturated model has greater pattern noise than a model with all saturation. So in terms of relative error, saturation improves the model performance for images 1 and 2. For Image 3, which has the lowest contrast,[29] it is seen that addition of saturation does not improve pattern noise. But when one compares the shape of the curves with the physiological data, to see if the peaks and troughs are seen at similar places as is tested using the cross covariance technique, it is found that the model with no saturation has more similarities than the one with saturation implemented.

In order to test the physiological data obtained, we have correlated the first half of the data with the second half. In a perfect physiological recording this should give us a value very close to 1. But we found that that self correlation results shows that physiological recording gives a lower value for the high contrast Image 1 compared to the low contrast Image 3 as seen in Table 3 which could be one reason why our model gives poor results.

Image 1 on itself	0.3380
Image 2 on itself	0.6169
Image 3 on itself	0.7359

Table 3. Cross correlation values obtained by correlating the first half of the image on the second half. In order to test the physiological data obtained, we have correlated the first half of the data with the second half. In a perfect physiological recording this should give us a value very close to 1. But we found that that self correlation results shows that physiological recording gives a lower value for the high contrast Image 1 compared to the low contrast Image 3 as seen in this table which could be one reason why our model gives poor results.

Window size	**Relative Error**	**Cross-Covariance**
2×2	0.7018	0.1282
4×4	0.6954	0.1369
8×8	0.6669	0.1553
16×16	0.6320	0.1725
32×32	0.5980	0.1796

Table 4. Relative error and cross covariance values at different window size. Testing Image 2 with different window widths, increasing the window width from just 2×2 square window to a 32×32 square window, using the model with no saturation, we calculated the relative error and cross covariance in each case as shown in this Table. It is seen that relative error decreases as the window size increases and there is better covariance with larger windows than there is with small window size showing that larger window of EMDs gives better results than small windows.

Testing Image 2 with different window widths, increasing the window width from just 2×2 square window to a 32×32 square window, using the model with no saturation, we calculated the relative error and cross covariance in each case as shown in the Table 4. It is seen that relative error decreases as the window size increases and there is better covariance with larger windows than there is with small window size showing that larger window of EMDs gives better results than small windows.

6. CONCLUSION

In this paper we study the pattern noise present in HS cell response and we attempt to reproduce pattern noise seen in the fly response using natural images with our model. The addition of static compressive non-linearity at different places in the model has been found to have a clear affect on the shape of the pattern noise and it is likely that saturation has a role in affecting pattern noise in the fly motion detector. But it is still not clear where this saturation mechanism occurs within the visual system of insects. This paper has explored the implementation of saturation at the input, at the correlator arms and at the output based on previous research carried out on the fly. But it could be that saturation may be present in other areas of the fly visual system and more study on the presence of saturation and combination of different kinds of saturation needs to be explored to make velocity response independent of the structure of the visual scene. It is also clear from the cross covariance results that there could be more non-linearities present in the insect eye which the model has failed to capture and hence more work needs to be carried out to get a reliable and perfect model of the insect eye capable of accurate velocity estimation. In nature, pattern noise is due to the response of local motion detectors to image features. It is largely reduced by the horizontally extended receptive field of HS cells and by summation at the steering muscles as is seen from our experiment using different window size. And our models are able to show this and can thus be used to predict the impact of pattern noise on artificial motion detectors.

Acknowledgments

This project was supported by US Air force for Scientific Research /AOARD (contract # F62562-01-P-0158) and US Air force SBIR contract (contract # F08630-01-C-0050).

REFERENCES

1. F. Ratliff and H. K. Hartline, *Studies on Excitation and Inhibition in Retina*, Chapman and Hall, London, 1974.
2. R. B. Pinter, "Adaptation of receptive field spatial organization via multiplicative lateral inhibition," *Proceedings of the the IEEE Conference on Systems, Man and Cybernetics* , pp. 328–331, 1984.
3. A. Bouzerdoum and R. B. Pinter, "Image motion processing in biological and computer vision systems," *Proceedings of the SPIE Conference on Visual Communications and Image Processing* **1199**, pp. 1229–1240, 1989.
4. G. A. Horridge, "A template theory to relate visual processing," *Proceedings of the Royal Society of London B* **239**, pp. 17–33, 1990.
5. P. Sobey, "Determining range information from self motion - the template model," *Proceedings of the SPIE on Intelligent Robots and Computer Vision* **1382**, pp. 123–131, 1990.
6. A. Moini, A. Bouzerdoum, A. Yakovleff, and K. Eshraghian, "A two dimensional motion detector based on insect vision," *Advanced Focal Plane Arrays and Electronic Cameras,* Berlin, Germany , pp. 146–157, October 1996.
7. A. Moini and A. Bouzerdoum, "A biologically motivated imager and motion detector with pixel level image processing," *Australian Microelectronics Conference,* Melbourne, Australia , pp. 180–185, 29 September-3 November 1997.
8. A. Moini, A. Bouzerdoum, K. Eshraghian, A. Yakovleff, X. T. Nguyen, A. Blanksby, R. Beare, D. Abbott, and R. E. Bogner, "An insect vision based motion detection chip," *IEEE Journal of Solid State Circuits* **32**, pp. 279–284, February 1997.
9. E. H. Adelson and J. Bergen, "Spatiotemporal energy models for the perception of motion," *Journal of the Optical Society of America A* **2**, pp. 284–299, 1985.
10. J. P. van Santen and G. Sperling, "Elaborated Reichardt detectors," *Journal of the Optical Society of America A* **2**, pp. 300–321, 1985.
11. F. Wolf-Oberhollenzer and K. Kirschfeld, "Motion sensitivity in the nucleus of the basal optic root of the pigeon," *Journal of Neurophysiology* **71**, pp. 1559–1573, 1994.
12. R. C. Emerson, M. C. Citron, W. J. Vaughn, and S. A. Klein, "Nonlinear directionally selective subunits in complex cells of cat striate cortex," *Journal of Neurophysiology* **58**, pp. 33–65, 1987.
13. B. Hassenstein and W. Reichardt, "Structure of a mechanism of perception of optical movement," *Proceedings of the 1st International Conference on Cybernetics* , pp. 797–801, 1956.
14. M. V. Srinivasan, S. W. Zhang, M. Lehrer, and T. S. Collet, "Honeybee navigation en route to the goal: visual flight control and odometry," *Journal of Experimental Biology* **199**, pp. 237–244, 1996.
15. S. P. McKee, G. H. Silverman, and K. Nakayama, "Precise velocity discrimination despite random variation in temporal frequency and contrast," *Vision Research* **26**, pp. 609–619, 1986.
16. M. Egelhaaf, A. Borst, and W. Reichardt, "Computational structure of a biological motion detection system as revealed by local detector analysis in the fly's nervous system," *Journal of the Optical Society of America A* **6**, pp. 1070–1087, 1989.
17. R. O. Dror, D. C. O'Carroll, and S. B. Laughlin, "Accuracy of velocity estimation by Reichardt correlators," *Journal of the Optical Society of America A* **18**, pp. 241–252, February 2001.
18. S. B. Laughlin, "Matching coding, circuits, cells and molecules to signals: general principles of retinal design in the fly's eye," *Progress in Retinal Research* **13**, pp. 165–195, 1994.
19. M. Egelhaaf and A. Borst, "Transient and steady state response properties of movement detectors," *Journal of the Optical Society of America A* **6**, pp. 116–127, 1989.

20. S. Single and A. Borst, "Dendritic integration and its role in computing image velocity," *Science* **281**, pp. 1848–1850, 1998.
21. K. Hausen and M. Egelhaaf, Neural mechanisms of visual course control in insects, *Facets in vision*, edited by R. Hardie and D. Stavenga, Springer-Verlag, Berlin, 1989.
22. T. Maddess and S. B. Laughlin, "Adaptation of the motion sensitive neuron h1 is generated locally and governed by contrast frequency," *Proceedings of the Royal Society of London B* **225**, pp. 251–275, 1985.
23. R. A. Harris, D. C. O'Carroll, and S. B. Laughlin, "Adaptation and the temporal delay filter of fly motion detectors," *Vision Research* **39**, pp. 2603–2613, 1999.
24. D. L. Ruderman, "The statistics of natural images," *Network: Computation in Neural System* **5**, pp. 517–548, 1994.
25. A. van der Schaaf and J. H. van Hateren, "Modelling the power spectra of natural images: Statistics and information," *Vision Research* **36**(17), pp. 2759–2770, 1996.
26. D. L. Ruderman, "Origins of scaling in natural images," *Vision Research* **37**(23), pp. 3385–3398, 1997.
27. R. O. Dror, D. C. O'Carroll, and S. B. Laughlin, "The role of natural image statistics in biological motion estimation," *Proceedings of the IEEE International Workshop on Biologically Motivated Computer Vision,* Seoul, Korea **1811**, pp. 492–501, 2000.
28. A. C. James, *White-Noise Studies in the Fly Lamina*. PhD thesis, Australian National University, 1990.
29. A. Straw, *Neural responses to moving natural scenes*. PhD thesis, University of Adelaide, Australia, 2004.
30. R. C. Hardie, "Functional organisation of the fly retina," *Progress in Sensory Physiology* **5**, pp. 1–80, 1985.
31. M. V. Srinivasan and M. Lehrer, "Spatial acuity of honeybee vision and its spectral properties.," *Journal of Comparative Physiology A* **162**, pp. 159–172, 1988.
32. M. F. Land, "Visual acuity in insects," *Annual Review of Entomolgy* **42**, pp. 147–177, 1997.
33. R. Payne and J. Howard, "Response of an insect photoreceptor: a simple log-normal model," *Nature* **290**, pp. 415–416, 1981.
34. J. H. Howard, A. Dubs, and R. Payne, "The dynamics of phototransduction in insects," *Journal of Comparative Physiology* **154**, pp. 707–718, 1984.
35. K. Hausen, "Motion sensitive interneurons in the optomotor system of the fly. the horizontal cells: Receptive field organisation and response characteristics," *Biological Cybernetics* **46**, pp. 67–79, 1982.
36. R. O. Dror, "Accuracy of visual velocity estimation by Reichardt correlators," Master's thesis, University of Cambridge, Cambridge, UK, 1998.
37. S. Rajesh, T. Rainsford, and D. C. O'Carroll, "Modelling pattern noise in responses of fly motion detectors to naturalistic scenes," *Proceedings of SPIE on Biomedical Applications of Micro- and Nanoengineering II* **5651**, pp. 160–173, 2004.